

## Josephson-junction arrays with long-range interactions

J. Kent Harbaugh and D. Stroud

*Department of Physics, Ohio State University, Columbus, Ohio 43210*

(Received 20 May 1997)

We calculate the current-voltage ( $IV$ ) characteristics of a Josephson-junction array with long-range interactions. The array consists of two sets of equally spaced parallel superconducting wires placed at right angles. A Josephson junction is formed at every point wherever the wires cross. We treat each such junction as an overdamped resistively shunted junction, and each wire segment between two junctions as a similar resistively shunted junction with a much higher critical current. The  $IV$  characteristics are obtained by solving the coupled Josephson equations numerically. We find that, for a sufficiently large number of wires, the critical current saturates at a finite value because of the wire inductance, in excellent agreement with experiment. The calculated  $IV$  characteristics also show a striking hysteresis, even though each of the individual junctions is *non-hysteretic*. The hysteresis results from a global redistribution of current flow on the upper and lower voltage branches, and is also in excellent agreement with experiment. [S0163-1829(97)04338-5]

### I. INTRODUCTION

Hybrid Josephson-junction arrays are systems made up of both Josephson junctions and extended superconducting objects, such as superconducting wires. Such arrays are expected to have a variety of interesting properties, because the phase of the superconducting order parameter should vary continuously in space within the extended regions, but should jump discontinuously between those regions.<sup>1</sup> An example of such an array is a collection of long superconducting wires. In such a system, small Josephson junctions form wherever two wires are sufficiently close to one another. In arrays of this kind, each wire, being long, is usually connected by a Josephson junction to a large number of other wires. For this reason, such arrays are sometimes said to have *long-range interactions*. Arrays of this kind were, to the best of our knowledge, first studied theoretically by Vinokur *et al.*<sup>2</sup> They have since been fabricated and studied both experimentally and theoretically by Sohn *et al.*<sup>3,4</sup> In the presence of a magnetic field, it has been predicted that such long-range interactions, even in periodic arrays, will give rise to glassy behavior.<sup>2,5,6</sup>

Other types of hybrid arrays can readily be imagined. For example, a hybrid system could be fabricated from a conventional two-dimensional Josephson-junction array by replacing all the junctions in one direction by superconducting wires. In three dimensions, a hybrid Josephson array might be constructed from a set of parallel superconducting planes, each of which has a periodic array of superconducting protrusions. Each protrusion, together with the corresponding protrusion from a neighboring plane, would form a small Josephson junction, while in the plane itself, the phase of the superconducting order parameter would vary continuously.

An ingenious theoretical method of treating hybrid Josephson arrays with long-range interactions was proposed by Vinokur *et al.*<sup>2</sup> In their picture, the superconducting order parameter in each wire is viewed as uniform, with a constant phase throughout the wire. The Josephson coupling between two given wires  $i$  and  $j$  is modeled by a coupling energy  $-J_{ij}\cos(\theta_i - \theta_j - A_{ij})$ , where  $\theta_i$  is the phase in the  $i$ th wire,  $J_{ij}$

is a coupling energy, and  $A_{ij}$  is a phase factor introduced to take account of an applied magnetic field. Since each wire thus interacts with a large number of other wires, the coupling Hamiltonian is treated by a generalization of a simple mean-field theory.<sup>7</sup> The resulting phase diagram has a number of interesting features, including a glasslike phase in a finite magnetic field.<sup>2,5,6</sup>

The experiments of Sohn *et al.* suggest that this approximation is oversimplified, in that it omits the inductance of the superconducting wires. In these experiments, two sets of parallel, equally spaced thin superconducting wires are arranged at right angles to one another. At each intersection between two wires, a small Josephson junction is formed. Current is then injected into one of the first set of parallel wires, and removed from a wire in the other set [see Fig. 1(a)]. If there were no inductance (i.e., if the phases along the wires were constant), the critical current  $I_c^{\text{array}}$  in this arrangement would be expected to be linear in the number of wires  $N$  in each parallel set. Instead, it is found that, for large  $N$ ,  $I_c^{\text{array}}$  saturates at a value much smaller than  $NI_c$ , where  $I_c$  is the critical current of a single junction. Sohn *et al.* attribute this discrepancy to the inductive response of the superconducting wires, a response that would be vanishingly small if the phase were constant along each wire.

In this paper, we describe a simple method of modeling the dynamics of Josephson arrays with long-range interactions, including the effects of wire inductance. The idea is simply to treat each wire segment between two Josephson point junctions as itself a Josephson junction, but with a much higher critical current. This model correctly includes the kinetic inductance of the wire segment, and also allows for the possibility of phase slips along the wire, which may occur in real superconducting wires. Since the critical current of the wire segments is high, the phase drop along any given wire segment between two junctions is usually small, so that the segment will generally behave like a pure inductance. We numerically solve the coupled Josephson equations for this model, and find that the  $IV$  characteristics closely resemble those seen experimentally. The critical current is linear in  $N$  for small  $N$ , but saturates at a finite value for large

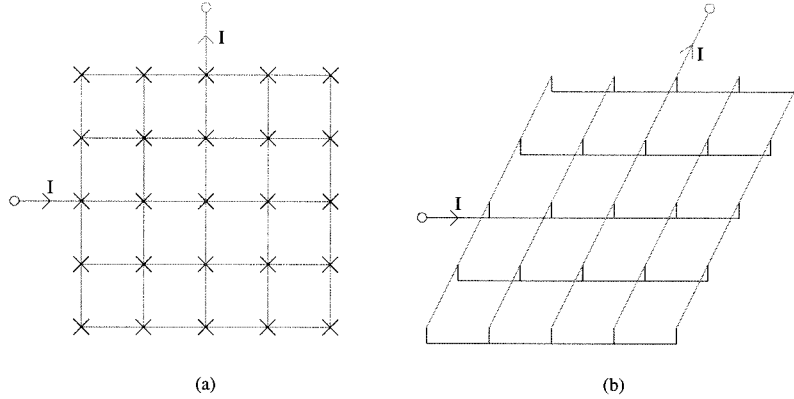


FIG. 1. Schematic of experimental geometry. (a) Top view, (b) perspective view. The array consists of two equally spaced sets of identical parallel wires, arranged perpendicular to one another. A vertical point junction is formed wherever two perpendicular wires cross one another. Current  $I$  is injected into the central wire in one set of parallel wires, and extracted from the central wire of the other set, as shown. In case of an even number of wires  $N$  in each layer, the current is injected just below center and extracted just left of center. Vertical junctions are modeled as overdamped resistively shunted Josephson junctions (RSJ's) with critical current  $I_c$  and resistance  $R$ . Horizontal segments in each layer are also modeled as overdamped RSJ's with critical current  $\lambda I_c$  and shunt resistance  $\mu R$ , where  $\lambda \gg 1$  and  $\mu \ll 1$  are dimensionless constants. The voltage drop is calculated between the input and output current terminals.

$N$ . The saturation value varies as the inverse square root of wire inductance per unit length. This is in excellent agreement with a simple model suggested by Sohn *et al.*,<sup>3,4</sup> and the occurrence of saturation is also confirmed experimentally.<sup>3,4</sup>

We also find that our numerical current-voltage ( $IV$ ) characteristics are *hysteretic*, even though the array, in our model, is composed entirely of *nonhysteretic* elements. Similar hysteresis was observed by Sohn *et al.*, who speculated that it resulted from differences in the patterns of current flow on increasing and decreasing the applied current. In our simulations, we are able not only to verify this speculation, but also to trace out the specific paths followed by the current on both branches of the hysteretic  $IV$  characteristic.

We turn now to the body of the paper. Section II describes our model for the long-range array. Our numerical results are given in Sec. III, followed by a brief discussion in Sec. IV.

## II. MODEL

The geometry of our array is shown in Fig. 1. The array consists of two sets of  $N$  parallel, equally spaced wires, arranged perpendicular to one another. A current  $I$  is fed into the center wire in one of the parallel set of wires, and removed from the center wire of the other [see Fig. 1(a)]. A Josephson junction is formed at each crossing point. We calculate the voltage drop between the input and output leads, as well as the voltage drop and current through each of the elements of the array. We can, in principle, also consider a magnetic field applied perpendicular to the array; the results of such calculations will be described elsewhere.

Our dynamical model for this system is quite simple. Each crossing point between two perpendicular wires [shown as a short vertical line in Fig. 1(b)] is modeled as an overdamped resistively shunted Josephson junction with critical current  $I_c$  and shunt resistance  $R$ . Each wire segment connecting two such junctions is itself modeled as an overdamped Josephson junction, with critical current  $\lambda I_c$  and

shunt resistance  $\mu R$ , where we expect  $\lambda \gg 1$  and  $\mu \ll 1$ . Clearly, a larger  $\lambda$  corresponds to a wire with a smaller inductance per unit length. Our model includes only the kinetic inductance of the wire, i.e., that associated with the motion of Cooper pairs, and ignores the electromagnetic part, which arises from magnetic fields produced (via Maxwell's equations) by the supercurrents flowing in the wire.

We describe the array by two phases at each vertical junction, corresponding to the points in each layer where two perpendicular wires cross one another [cf. Fig. 1(b)]. Thus, for two sets of  $N$  perpendicular wires, there are  $2N^2$  phases. The current  $I_{ij}$  flowing from point  $i$  to point  $j$  is taken as that of an overdamped resistively shunted junction:

$$I_{ij} = I_{cij} \sin(\theta_i - \theta_j - A_{ij}) + \frac{\hbar}{2eR_{ij}} (\dot{\theta}_i - \dot{\theta}_j - \dot{A}_{ij}). \quad (1)$$

Here  $I_{cij}$  is the critical current for the  $(ij)$ th Josephson junction, the overdot denotes a time derivative, and

$$A_{ij} = \frac{2e}{\hbar c} \int_i^j \mathbf{A} \cdot d\mathbf{l} \quad (2)$$

is a phase factor that takes account of any applied magnetic field ( $\mathbf{A}$  being the vector potential describing that field). The first term on the right-hand side is the Josephson current through junction  $ij$ , while the second term is the current through the shunt resistance,  $V_{ij}/R_{ij}$ .  $V_{ij}$  is the instantaneous voltage between points  $i$  and  $j$  and we have used the Josephson relation  $V_{ij} = (\hbar/2e)(\dot{\theta}_i - \dot{\theta}_j - \dot{A}_{ij})$ . The dynamical description is completed by Kirchoff's equations of current conservation:

$$I_i^{\text{ext}} = \sum_{i \neq j} I_{ij}, \quad (3)$$

where  $I_i^{\text{ext}}$  is the external current fed into point  $i$ . In the geometry of Fig. 1(b),  $I_i^{\text{ext}} = \pm I$  at the input and output terminals, and zero everywhere else.

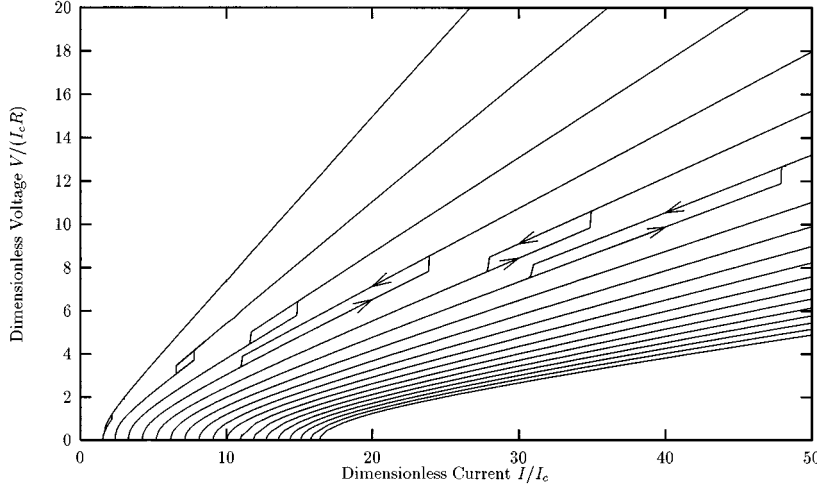


FIG. 2. Current-voltage ( $IV$ ) characteristics for arrays of sizes  $N=2$  to 19 (increasing from left to right) with the inverse inductance parameter  $\lambda=100$ . In the hysteretic regions, arrows indicate that the voltage is measured as the current is being increased from zero, or decreased from a high value.

We solve the equations of motion iteratively, using an adaptive step size, embedded 5(4) fixed-order Runge-Kutta-Fehlberg algorithm, as described, for example, by Cash and Karp.<sup>8</sup> Our method is similar to that employed by many others to calculate the  $IV$  characteristics and other dynamical properties of more conventional Josephson arrays.<sup>9</sup> In order to calculate time-averaged voltages we typically average over a period of  $1000t_0$  for each current after first allowing  $100t_0$  for equilibration, where  $t_0 = \hbar/(2eI_c R)$  is a natural unit of time.

In order to obtain  $IV$  characteristics, we start at zero applied current, then gradually ramp up the current in steps of order  $0.1I_c$  (but as small as  $0.01I_c$  in the transition region), up to some maximum value well above the transition. Following this gradual increase, we ramp the current down in the same steps. In each case, we always use the final phase configuration of the previous current as the initial state for the next current. In our calculations, we have considered various values of the inductance parameter  $\lambda$  ranging from 10 to 100, but have studied only the single resistance parameter  $\mu=0.01$ .

### III. RESULTS

Figure 2 shows the calculated  $IV$  characteristics for arrays of various sizes, plotted for  $\lambda=100$ . These curves suggest several typical features, all of which are shown with more precision in later figures. First, the critical current tends to increase with increasing array size, but saturates for large  $N$ . Second, there is a striking hysteresis in the  $IV$  characteristics. That is, for each size  $N$ , there is a range of current within which the voltage takes on *two* values. Of these, the larger of the two corresponds to *decreasing* (ramping down) the current. This hysteresis occurs even though the individual junctions themselves are overdamped, and therefore *nonhysteretic*. This hysteresis occurs for all value of  $N$ , though for  $N \geq 7$  the hysteretic region occurs outside the plotted current range. Some possible reasons for this hysteresis are discussed below.

The saturation of  $I_c^{\text{array}}$  is shown more quantitatively in Fig. 3, where we plot  $I_c^{\text{array}}$  for several values of  $\lambda$ . In each case,  $I_c^{\text{array}}$  is *linear* in  $N$  for small  $N$ , but saturates for large  $N$ . To an excellent approximation, the saturation value of

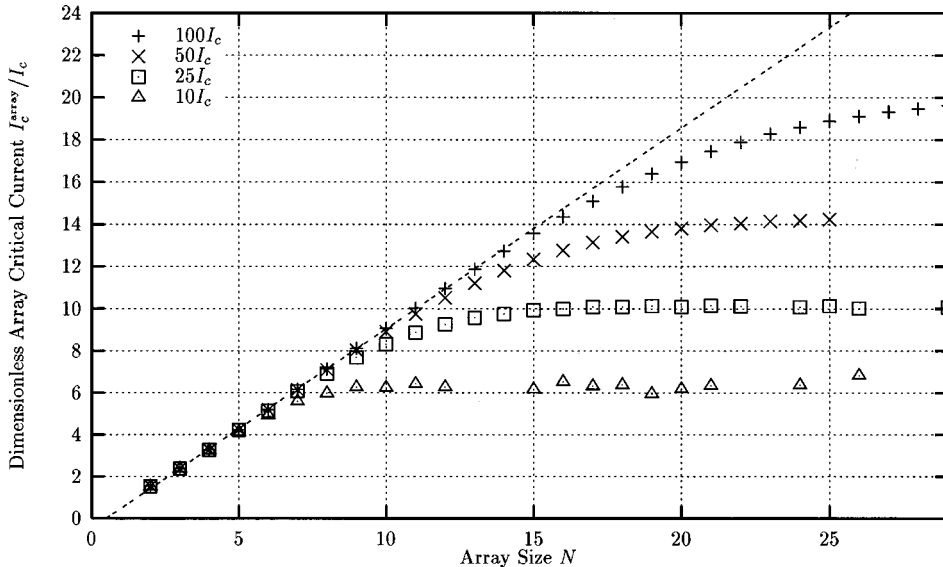


FIG. 3. Critical current  $I_c^{\text{array}}$  as a function of number of wires  $N$  in each layer, plotted for several  $\lambda=100, 50, 25,$  and  $10$  as indicated. The straight line has slope  $I_c$ , the critical current of a single vertical junction.

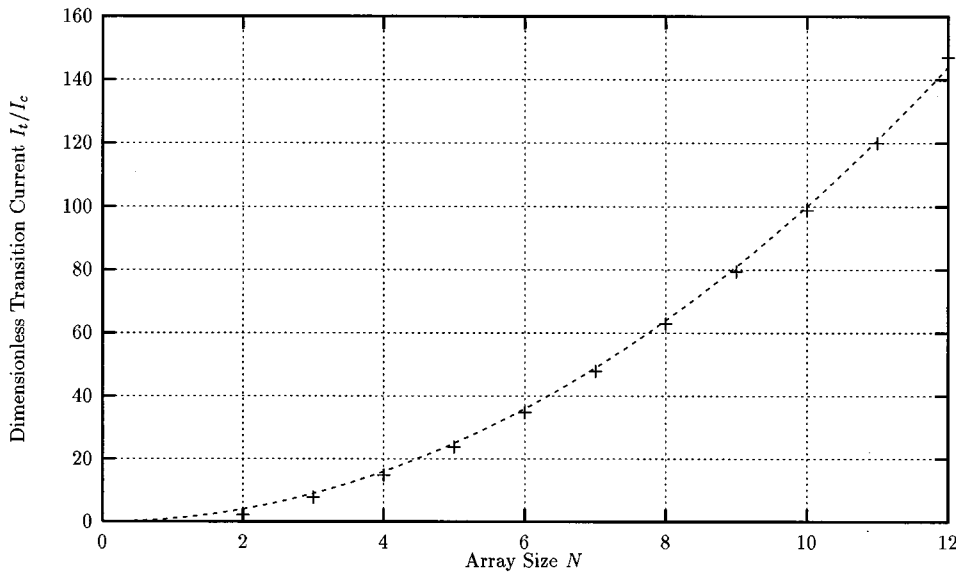


FIG. 4. Dimensionless transition current  $I_t/I_c$ , plotted as a function of  $N$  for an array in which  $\lambda = 100$ . Dashed line represents  $I_t/I_c = N^2$ ; crosses are calculated points.

$I_c^{\text{array}}$  is proportional to  $1/\sqrt{\lambda}$ . This behavior agrees perfectly with the simple analytical model proposed by Sohn *et al.*,<sup>3,4</sup> in which the wires are simply assumed to have a constant inductance per unit length (arising from a combination of kinetic and electromagnetic inductance). Thus, it is apparently quite satisfactory to treat the inductive response of the wires by modeling them as Josephson junctions with large critical currents. Our predicted saturation behavior also agrees with the experiments reported in Ref. 3. Specifically, in their  $1000 \times 1000$  arrays, they observe a critical current far smaller than  $NI_c$ . The linear behavior we predict for  $I_c^{\text{array}}$  at small  $N$  has not been tested experimentally, however, nor has the proportionality to  $1/\sqrt{\lambda}$ .

The hysteresis seen in Fig. 2 is generally a reproducible phenomenon in our calculations. We have found that the current of the upper discontinuity (which we will call the “transition current”  $I_t$ ) is quite insensitive to the rate at which the current is ramped up. The lower drop, however, does appear to depend on the history of the current sweep.

To an excellent approximation  $I_t = I_c N^2$ , as is shown in Fig. 4, which is simply the sum of the critical currents of all the vertical junctions. This result suggests that the transition corresponds to a global redistribution of current flowing through the array, as we have indeed confirmed by numerically evaluating the current and voltage drop across each junction and wire segment in the array. The resulting picture of the hysteresis, confirmed by these numerical checks, is the following. As the current is ramped up, it passes through the various vertical junctions. At any current above  $I_c^{\text{array}}$  but below  $I_t$ , the finite observed voltage is due entirely to voltage drops along two central paths along the wires of the input and output current [see Fig. 5(a), where we show this pattern for  $N = 5$ ]. Just below  $I_t$ , the current flowing through some of the vertical junctions that are off this central path start to reach  $I_c$ . At this point, there is a jump in time-averaged voltage, and also a global redistribution of current in the array. On this upper voltage branch, the voltage drop is nonzero across *all* the vertical junctions, as shown in Fig. 5(b).

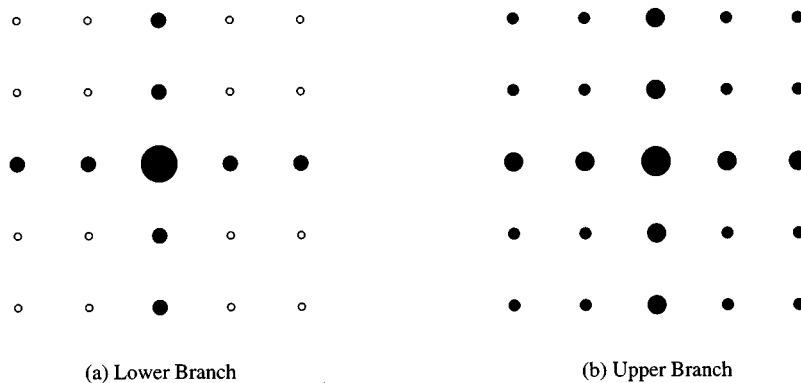


FIG. 5. Illustration of the different voltage patterns associated with points on the upper and lower voltage branches of Fig. 2, for  $N = 5$ . (a) and (b) show the voltage pattern at a current  $20I_c$ , for  $N = 5$  on the lower and upper voltage branches at a current in the bistable regime. The area of each filled circle is proportional to the current flowing through the vertical junction. Empty circles correspond to a zero voltage drop across the junction. On the lower branch, all the voltage drop occurs on two lines extending along the input and output wires. On the upper branch, all the vertical junctions have nonzero voltage drops.

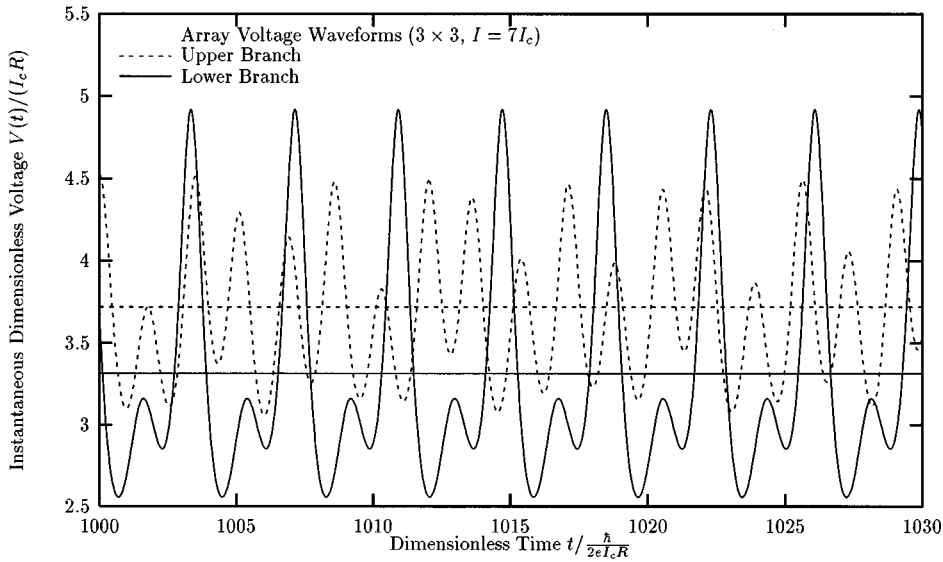


FIG. 6. Typical time-dependent voltage differences  $V(t)$  between input and output terminals for a current  $I=7I_c$  and  $N=3$ . Dashed line, a voltage on the lower branch; solid line, upper branch. The horizontal lines denote time-averaged voltage differences on each branch.

At high input currents, for all  $N$  we have considered, we find numerically that the voltage across the array takes the form  $IR_N$ , where to an excellent approximation,  $R_N=R[(2N-1)/N^2]$ . We have verified analytically (by solving Kirchhoff's laws) that this is precisely the effective resistance of a network of  $N^2$  resistors, each of resistance  $R$  and arranged in this geometry. On the lower voltage branch, at input currents below the array transition current but above  $I_c^{\text{array}}$ , we find numerically that the array voltage is given by

$$V \approx \frac{2}{N+1} R \sqrt{I^2 - I_c^{\text{array}2}}. \quad (4)$$

This has the same form as the voltage of a single junction of critical current  $I_c^{\text{array}}$  and shunt resistance  $2R/(N+1)$ , but we have not succeeded in deriving this result analytically. Nonetheless, the use of this form along with  $I_t \approx I_c N^2$ , allows us to estimate the voltage discontinuity at  $I_t$  as  $\Delta V_t \approx I_c R(N-1)/(N+1) \approx I_c R$  for large  $N$ . The voltage discontinuities measured in Ref. 3 appear to be of approximately this magnitude.

Not surprisingly, the voltages on the upper and lower voltage branches have quite different time-dependences. As an example, Figs. 6(a) and 6(b) show time traces of the voltage  $V(t)$  between the input and output terminals in an  $N=3$  array at the same current but for points on the upper and lower voltage branches. On the lower branch, the signal appears to be periodic, but with several conspicuous harmonics in addition to the fundamental. On the upper branch,  $V(t)$  is considerably more complex and seemingly aperiodic. The precise origins of this behavior are not clear. For larger  $N$ , the time-dependent voltages also differ on the two branches but are both considerably more complex than shown in Fig. 6.

#### IV. DISCUSSION

We have presented a simple model to describe the behavior of hybrid Josephson-junction arrays consisting of two

sets of parallel superconducting wires, arranged at right angles. In our model, the inductance of the wires is treated by modeling each wire segment as an overdamped Josephson junction of critical current much larger than that of the vertical junctions. The  $IV$  characteristics of the array can then be calculated simply by solving the coupled resistively shunted junction equations numerically. The resulting  $IV$  behavior is in excellent agreement with experiment, suggesting that our simple approach to wire inductance is adequate for this problem. In particular, our calculated critical current saturates for large  $N$ , as observed experimentally; the saturation value is proportional to the inverse square root of the wire kinetic inductance. Furthermore, our calculations lead to an array that is found to be *hysteretic*, even though every element in the array is individually *nonhysteretic*. We have shown that the hysteresis arises from a global redistribution of the current flow pattern in the array. In the hysteretic regime, there are two different metastable voltage patterns, corresponding to two very different patterns of current flow.

The present model can be extended in a variety of ways. Because of the disorder in a realistic array, the vertical junctions will certainly have a random distribution of critical currents, rather than a unique critical current as assumed here. Presumably, this distribution would produce a whole series of jumps and hysteretic regimes in the  $IV$  characteristic, rather than the single hysteretic region found here. Such a series of jumps is apparent in the published experimental data. The present model can also be readily extended to include a finite external magnetic field. Such a field is found experimentally to produce a wide range of effects in both the static and dynamical properties of such arrays. We plan to discuss our finite field results in a future publication.

#### ACKNOWLEDGMENTS

This work has been supported by NSF Grant No. DMR 94-02131 and by the Midwest Superconductivity Consortium at Purdue University through DOE Grant No. DE-FG02-90-45427.

- <sup>1</sup>See, for example, M. Basler, W. Krech, and K. Y. Platov, *Phys. Rev. B* **55**, 1114 (1997), and references cited therein.
- <sup>2</sup>V. M. Vinokur, L. B. Ioffe, A. I. Larkin, and M. V. Feigel'man, *Zh. Éksp. Teor. Fiz.* **93**, 343 (1987) [*Sov. Phys. JETP* **66**, 198 (1987)].
- <sup>3</sup>L. L. Sohn, M. T. Tuominen, M. S. Rzchowski, J. U. Free, and M. Tinkham, *Phys. Rev. B* **47**, 975 (1993).
- <sup>4</sup>L. L. Sohn, M. S. Rzchowski, J. U. Free, and M. Tinkham, *Phys. Rev. B* **47**, 967 (1993).
- <sup>5</sup>P. Chandra, L. B. Ioffe, and D. Sherrington, *Phys. Rev. Lett.* **75**, 713 (1995).
- <sup>6</sup>P. Chandra, M. V. Feigel'man, and L. B. Ioffe, *Phys. Rev. Lett.* **76**, 4805 (1996).
- <sup>7</sup>W. Y. Shih and D. Stroud, *Phys. Rev. B* **28**, 6575 (1983).
- <sup>8</sup>J. R. Cash and Alan H. Karp, *ACM Trans. Math. Softw.* **16**, 201 (1990).
- <sup>9</sup>See, e.g., S. R. Shenoy, *J. Phys. C* **18**, 5163 (1985); K. K. Mon and S. Teitel, *Phys. Rev. Lett.* **62**, 673 (1989); J. S. Chung *et al.* *Phys. Rev. B* **40**, 6570 (1989); D. Dominguez and J. V. José, *Int. J. Mod. Phys. B* **8**, 3749 (1994), and references cited therein.